

Cosmology in a nutshell + an argument against $\Omega_\Lambda = 0$ based on the inconsistency of the CMB and supernovae results

Charles H. Lineweaver

University of New South Wales, Sydney, Australia

Abstract. I present several simple figures to illustrate cosmology and structure formation in a nutshell. Then I discuss the following argument: if we assume that $\Omega_\Lambda = 0$ then the CMB results favor high Ω_m while the supernova results favor low Ω_m . This large inconsistency is strong evidence for the incorrectness of the $\Omega_\Lambda = 0$ assumption. Finally I discuss recent CMB results on the slope and normalization of the primordial power spectrum.

1 Cosmology in a nutshell

The Big Bang model became the standard cosmological model soon after the discovery of the cosmic microwave background (CMB). The Big Bang model has a hot, dense early epoch (see Figure 1) when nucleosynthesis occurred. It also has an opaque surface that can naturally produce the Planckian spectrum of the CMB. The Steady State universe was not hotter in the past, has no epoch of Steady State Nucleosynthesis and has no opaque surface to produce the CMB.

Gravitational collapse is the leading model of structure formation (Figure 2). Slight over-densities are gravitationally unstable and collapse under their own self-gravity. In an alternative family of models, structure forms from topological defects. In gravitational collapse models CMB anisotropies larger than ~ 1 degree are acausal and rely on inflation to explain their existence. In defect models these large anisotropies are close by, causal and sub-horizon sized.

Figure 1. Big Bang vs Steady State. Expanding horizon volumes in the Big Bang (A) and Steady State (B) models. The dots represent the density of the Universe. At early times only the Big Bang model was dense and hot providing an oven for nucleosynthesis and later an opaque surface of last scattering which naturally produces the Planckian spectrum of the CMB.

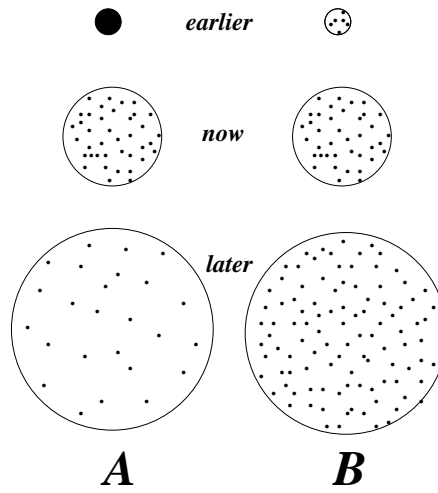
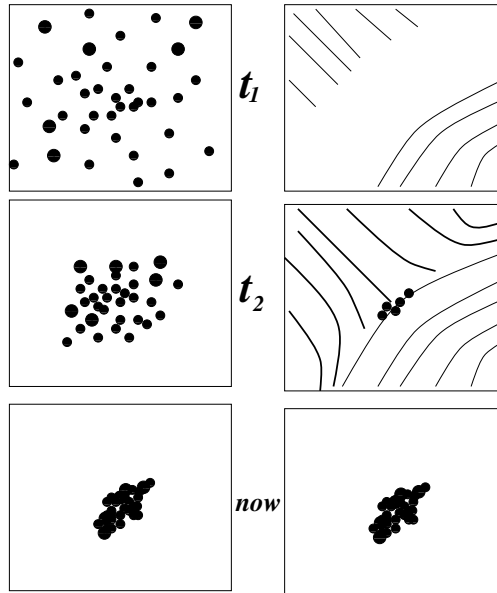


Figure 2. Gravitational collapse vs topological defects. The leading model of structure formation is on the left: small over-densities are gravitationally unstable and collapse under their own gravity to form the structures we see around us. Topological defect models (right) are an alternative. When symmetry is broken in the early universe causally disconnected regions are occupied by different vacuum states (indicated by the direction of the lines in the figure). Large energy densities are present at the boundaries between such regions and this is where structure forms.



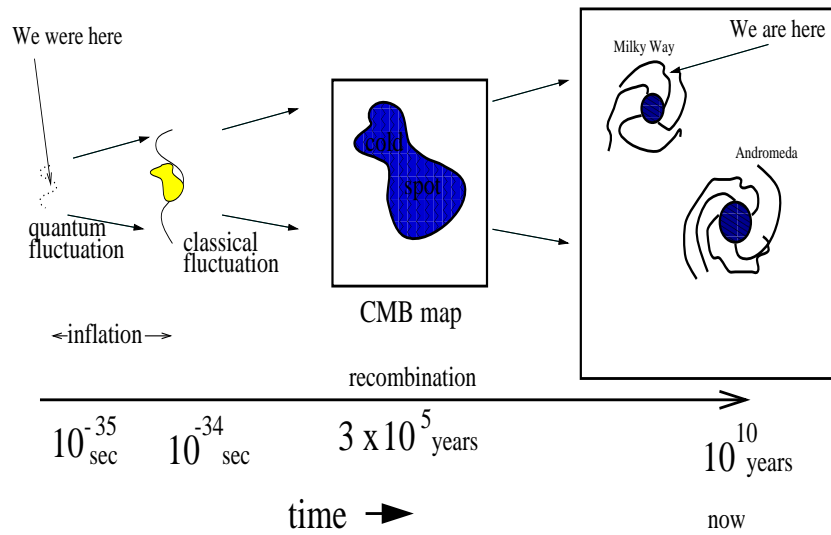


Fig. 3. Galaxies are CMB anisotropies are Quantum fluctuations. According to the inflationary scenario, quantum fluctuations of a scalar field are the origin of all structures. These quantum fluctuations are not caused by any preceding event in the same sense as radioactive decay or quantum tunneling are not caused. They are non-deterministic prime movers. Inflation of the universe by a factor of more than 10^{26} transforms these quantum fluctuations into super-horizon classical density fluctuations. On their way to becoming galaxies we can monitor their progress by looking at CMB maps.

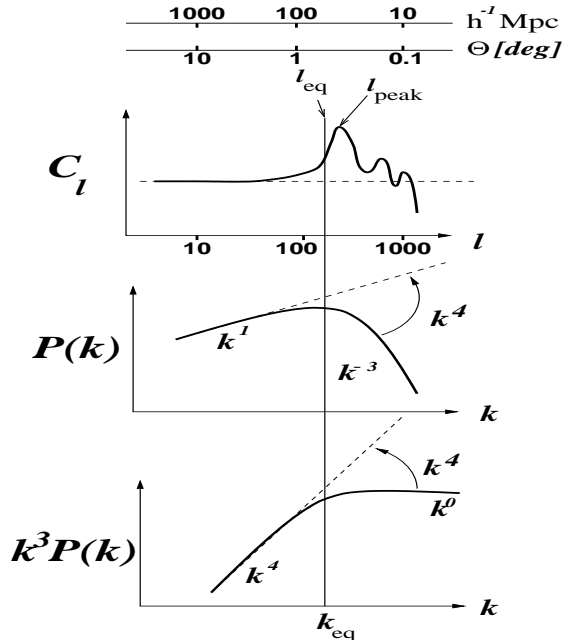
One of the most important questions in cosmology is: What is the origin of all the galaxies, clusters, great walls, filaments and voids we see around us? The inflationary scenario provides the most popular explanation for the origin of these structures: they used to be quantum fluctuations.

Figure 3 illustrates the metamorphosis of quantum fluctuations to CMB anisotropies to galaxies. Primordial quantum fluctuations of a scalar field get amplified and evolve to become classical seed perturbations and eventually large scale structure. This process can be monitored by CMB observations since matter fluctuations produce temperature fluctuations in the CMB: $\frac{\delta\rho}{\rho} \propto \frac{\Delta T}{T}$.

How does a particular fluctuation know whether it will become a spiral or an elliptical galaxy? Does the density and irregularity of its environment determine its morphology by controlling its angular momentum and the amount of merging? With a full understanding of galaxy formation we may be able to look at CMB cold spots and their neighborhoods and predict where they will end up in the Hubble tuning fork diagram of galaxy types. The distribution of morphological types at high redshift discussed by Driver in these proceedings would then be a derivable function of the characteristics of the CMB anisotropies.

Figure 4.

CMB powerspectrum (C_ℓ , top) compared with the matter density powerspectrum ($P(k)$, middle and bottom). C_ℓ is a measure of the power in the spatial variations of the CMB as a function of the angular scale. The upper axes give the angular scales and comoving sizes corresponding to the Legendre polynomial index ℓ . In the bottom two panels the turnover in $P(k)$ at $\sim k_{eq}$ occurs at the scale ($L_{eq} = 2\pi k_{eq}^{-1}$) which just enters the horizon as the Universe changes from radiation dominated to matter dominated. Smaller sizes entered the horizon earlier during radiation domination and were unable to grow during this period. The k^4 growth suppression which they suffered is indicated.



1.1 There is no scale beyond which the universe is homogeneous

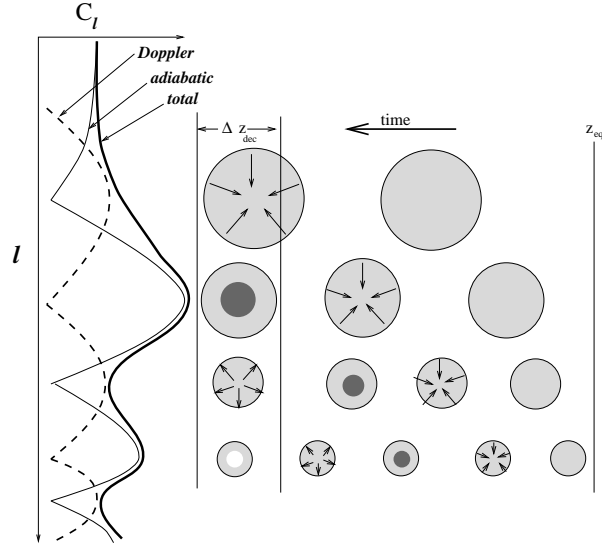
It has been claimed that some recent, deep, galaxy redshift surveys have reached the scale at which the Universe becomes homogeneous. Strictly speaking however there is no scale beyond which the universe is homogeneous. The amplitude of the density contrast ($\delta\rho/\rho \propto k^3 P(k)$) decreases for larger scales but is never zero. A more meaningful question is: Where is the turnover in the power spectrum? This turnover is due to a suppression of growth of a given k mode by k^4 relative to modes which enter the horizon during matter domination (assuming $\Omega_o = 1$). Thus, the horizon scale at matter-radiation equality is an important diagnostic of this fundamental scale. See Figure 4.

Lineweaver & Barbosa (1998) have used current CMB anisotropy measurements to determine the position of the adiabatic peak in the CMB spectrum under the assumption of open or critical density CDM dominated universes: $\ell_{peak} = 260^{+30}_{-20}$.

Figure 5 illustrates how harmonic sound bumps appear in the CMB power spectrum driven by the wells and valleys of the CDM potentials. The epoch when matter and radiation densities are equal has a redshift of z_{eq} while decoupling occurs at z_{dec} . The number of oscillations between z_{eq} and z_{dec} and thus the phase of the oscillations at z_{dec} is determined by i) the physical size of the potential well, ii) the speed of sound and iii) the time interval between z_{eq} and z_{dec} .

Figure 5.

Sound waves in the photon-baryon fluid create bumps in the CMB power spectrum. The grey spots are cold dark matter potential wells which initiate infall and then oscillation of the photon-baryon fluid in these wells. The Doppler and adiabatic effects make the sound visible in the radiation when the baryons decouple from the photons during the interval marked Δz_{dec} . These bumps are analogous to the standing waves of the resonant frequencies of a plucked string or of a good shower and may be the oldest music in the Universe. See Hu *etal* (1997) and Lineweaver (1997) for details.

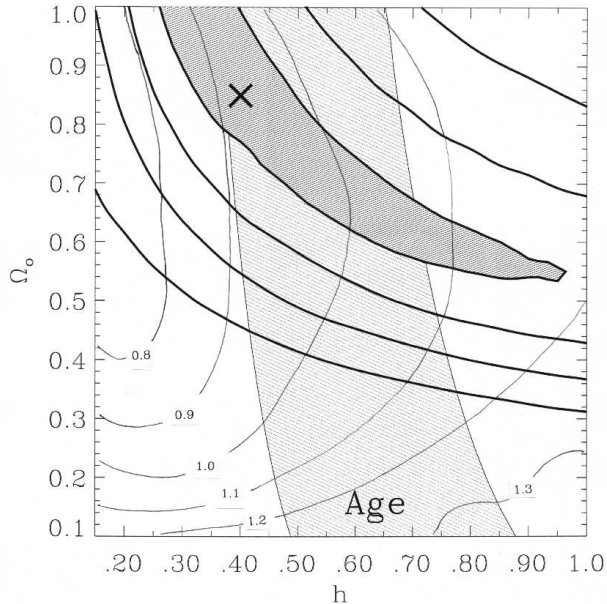


2 An argument against $\Omega_\Lambda = 0$ based on the inconsistency of the latest CMB and supernovae constraints on Ω_m .

The CMB is already giving us useful constraints on cosmological parameters in popular but restricted families of CDM models. In Figure 6 the region of the $h - \Omega_m$ plane preferred by the CMB data is shown (since $\Omega_\Lambda = 0$, $\Omega_0 = \Omega_m$). The best-fit is indicated with an **X**. The values of the spectral index n which minimize the χ^2 values for a given (h, Ω_o) pair are indicated by the thin solid iso- n lines and are labeled with 0.8 – 1.3. High values of h require high values of n .

Figure 6.

The dark grey banana-shaped region is the approximate 68% confidence level preferred by the current CMB anisotropy measurements. The thick solid lines are the approximate 2, 3 and 4 σ contours. The age interval shown is 10 – 18 Gyr. The thin lines are contours of the spectral index n values which minimize the χ^2 for each pair (h, Ω_o) . Note the monotonic relations: the higher the h value the higher the n value and the lower the Ω_o value. A favored open model $h \approx 0.70$ with $\Omega_o \approx 0.3$ is rejected at greater than $\sim 4\sigma$. The best-fit value is $h = 0.40$ and $\Omega_o = 0.85$. The corresponding n value is 0.91. Figure adapted from Lineweaver & Barbosa (1998).



Under the assumption that $\Omega_\Lambda = 0$ (i.e., $\Omega_o = \Omega_m$) the most recent CMB results on the density of matter in the Universe yield $\Omega_m > 0.3$ at the $\sim 4\sigma$ confidence level (Figure 6). This result is independent of the value of Hubble's constant, of the spectral index n and of the normalization Q_{10} . In this same model the new supernovae results are $\Omega_m = -0.1 \pm 0.5$ (Garnavich *et al.* 1998) and $\Omega_m = -0.4 \pm 0.1$ (statistical) ± 0.5 (systematic) (Perlmutter *et al.* 1998). With additional supernovae Ω_m stays low and the error bars decrease making the inconsistency between CMB and supernovae results even stronger (Schmidt 1998 private communication). People who like open models with $\Omega_\Lambda = 0$ could argue that these supernovae results are consistent with some cosmological measurements which yield $0.1 \lesssim \Omega_m \lesssim 0.3$. However the strong inconsistency between

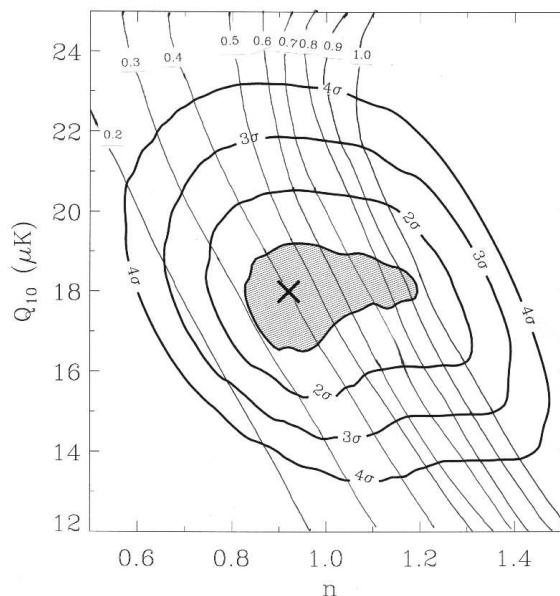
the CMB results (which strongly exclude low values of Ω_m) and the supernovae which favor very low, even negative (and thus unphysical) values of Ω_m is strong evidence against $\Omega_\Lambda = 0$ models.

3 Results for the slope and normalization of the CMB power spectrum

The CMB solutions for h or n can be read from either Figure 6 or 7. CMB anisotropy measurements in open and critical CDM models yields $n = 0.91^{+0.29}_{-0.09}$ (Lineweaver & Barbosa 1998). In Figure 7 the thin solid lines indicate the h values ($0.2 \leq h \leq 1.0$) which minimize the χ^2 for (n, Q_{10}) pairs. Conditioning on $n = 1$ or $h = 0.50$ changes the results (see Table 2 of Lineweaver & Barbosa 1998).

Figure 7.

Contours in the plane of the slope n and normalization Q_{10} of the primordial power spectrum of CMB anisotropies. Notation is analogous to the previous figure except here the thin lines are contours of the h values which minimize the χ^2 for a given pair of (n, Q_{10}) . Note the monotonic relation: for a given Q_{10} value, the higher the n value the higher the h value. The best-fit values of n and Q_{10} are $n = 0.91^{+0.29}_{-0.09}$ and $Q_{10} = 18.0^{+1.2}_{-1.5}$. To my knowledge, these are the tightest constraints on these parameters. Figure adapted from Lineweaver & Barbosa (1998).



References

- Garnavich, P.M. *et al.* 1998 *Astrophysical Journal*, submitted, astro-ph/9710123
 Hu, W., Sugiyama, N. & Silk, J (1997) *Nature*, 386, 37
 Lineweaver, C.H. 1997, in "From Quantum Fluctuations to Cosmological Structures",
 ed. D. Valls-Gabaud, M.A.Hendry, P. Molaro & K. Chamcham, ASP conference
 series, 126, p 185-205
 Lineweaver, C.H., Barbosa, D. (1998), *Astrophysical Journal*, 496, (in press), astro-
 ph/9706077
 Perlmutter, S. *et al.* 1998, [http://panisse.lbl.gov/public/papers/aasposter198dir/
 /wwwposter2c2.jpg](http://panisse.lbl.gov/public/papers/aasposter198dir/wwwposter2c2.jpg)